International Journal of Mechanical, Industrial and Aerospace Sciences
ISSN: 2517-9950
Vol:3, No:5, 2009

A Refined Energy-Based Model for Friction-Stir Welding

Samir A. Emam, Ali El Domiaty

Abstract**—**Friction-stir welding has received a huge interest in the last few years. The many advantages of this promising process have led researchers to present different theoretical and experimental explanation of the process. The way to quantitatively and qualitatively control the different parameters of the friction-stir welding process has not been paved. In this study, a refined energy-based model that estimates the energy generated due to friction and plastic deformation is presented. The effect of the plastic deformation at low energy levels is significant and hence a scale factor is introduced to control its effect. The predicted heat energy and the obtained maximum temperature using our model are compared to the theoretical and experimental results available in the literature and a good agreement is obtained. The model is applied to AA6000 and AA7000 series.

Keywords**—**Friction-stir welding, Energy, Aluminum Alloys.

I. Introduction

THE energy required to bond two components by welding is usually provided by direct heat. The two common sources of direct heat are those derived from either a chemical reaction or electrical energy. The exception includes explosive bonding, which uses the kinetic energy released from the impact of a moving object with a stationary target and friction-stir welding, which combines frictional heating at the interface with the localized plastic deformation within the material.

Friction-stir welding (FSW) is a solid-state joining process that enables welding hard-to-wild metals such as high-strength aluminum alloys. Friction-stir welding was developed and patented by The Welding Institute (TWI) in 1991 [1]. Since then the research efforts to understand the micro and macromechanics of the process are continuous. During FSW, no melting point occurs, and as a result the process is performed at much lower temperatures than conventional welding processes. This has a direct impact on the safe application of the FSW to the environment. Among the advantages of the FSW are [2]

- Low distortion, even in long welds
- Excellent mechanical properties as proven by fatigue, tensile and bend tests
- No arc
- No fume
- No porosity
- No spatter
- Low shrinkage
- Energy efficient
- Non-consumable tool; one tool can typically be used for up to 1000m of weld length in 6000 series aluminum alloys
- No filler wire
- No gas shielding for welding aluminum
- No grinding, brushing or pickling required in mass production
- Can weld aluminum and copper of more than 50mm thickness in one pass.

However, as of the present time, there are some limitations, which include

- Workpieces must be rigidly clamped
- Backing bar required, when self-reacting tool or directly opposed tools are not available.
- Keyhole at the end of each weld.
- Cannot make joints which require metal deposition (e.g. fillet welds)

Friction-stir welding is carried out using a rotating tool that is attached to a shoulder piece and the whole unit is translating over the line of welding. The rotation and translation of the pin within and on top of the line of welding generates heat, which is used to weld the workpieces. Heat is generated due to plastic deformation of the workpiece and the effect of the friction between the surfaces of the tool and the workpiece [3, 4]. Figure 1 is a schematic of the friction stir welding process.

According to most of the literature, the weld zone around the tool is divided into four regions: unaffected or parent metal, heat affected zone (HAZ), thermo-mechanically affected zone (TMAZ), and weld nugget. The unaffected material is remote from the weld, which has not experienced deformation or it may have healed after being experienced a thermal cycle. The heat affected zone (HAZ), which was previously referred to as thermally affected zone, is in the neighborhood of the weld center and its microstructure and mechanical properties have been modifies as a result of experiencing a thermal cycle. This zone does not associate a plastic deformation. Thermo-mechanically affected zone (TMAZ) is plastically deformed due to the friction-stir welding tool and its microstructure is modified due to the generated heat. Finally, the weld-nugget zone is the

Samir Emam is with the Department of Mechanical Engineering, United Arab Emirates University, P.O. Box 17555, Al Ain, UAE; e-mail: semam@uaeu.ac.ae.

Aly El Domiaty, Department of Mechanical Engineering, Suez Canal University, Port Said, Egypt.

recrystallized area in the TMAZ.

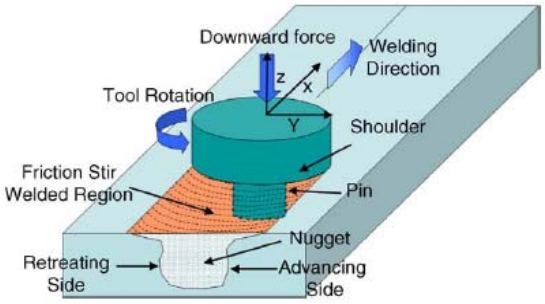

Fig. 1 A schematic of friction-stir welding process.

Modeling of FSW was presented by many authors. Bendzsak [5] used the finite volume method to compute the flow of the workpiece around the tool. Askari et al. [6] used an elasto-visco plastic model to estimate the material flow around the tool. A thermo-mechanical model was presented by Heurtier et al. [7] who analytically determined the flow pattern around the tool in order to calculate the effective strain in the deformed plastic zone. To achieve the same purpose, the finite element method [8-10] and the finite difference method [11] were used.

In the present work, a simple energy-based model for the friction stir weld is proposed. The model aims at estimating the heat generated due to plastic deformation within the work-pieces and friction between the tool surfaces and the work-pieces. This generated energy and the associated maximum temperature are compared to the results available in the literature to verify the proposed model.

II. The Proposed Energy Model

Previous studies [3] assume that heat generated due to friction of the pin shoulder on the workpiece surface is dominant and the heat generated due to the plastic deformation within the workpiece and the friction of the pin of the material is negligible. However, other authors e.g. Heurtier et al. [3] and Hamilton et al. [12] consider the heat generated from both the friction of the pin shoulder and plastic flow. In fact, the energy due to plastic deformation and friction of the shoulder with the surface of the workpiece are related and competing each other. As the heat generated by the shoulder is low, the flow stress is higher and hence the resulting plastic-deformation energy increases. On the other hand, as the heat generated by the shoulder is high, the flow stress reduces and as a result the plastic strain contribution decreases. In this work, heat is modeled to be generated by the friction of the shoulder and plastic deformation.

Figure 2 presents a schematic of the friction-stir welding tool. It is assumed that the tool rotates with an angular speed of ω and transversely translates along the line of welding with a speed of v_o. The tool is acted upon by a compressive force F, as shown in the figure.

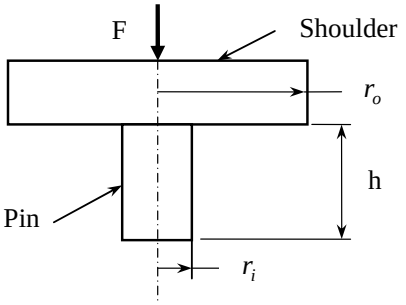

Fig. 2 Geometry of the FSW tool

Following, Hamilton et al. [12], the energy generated per unit length of the weld E is given by

$$E_f = P_f / v_o \qquad (1)$$

where P is the total power generated by friction. Assuming that the total torque due to friction of the pin, shoulder, and pin circumference with the workpiece surfaces is T_f, the frictional power is then given by

$$P_f = T_f \omega \qquad (2)$$

where ω is the pin angular speed. To find an expression for the total frictional torque T_f, we let

$$T_f = T_s + T_p \qquad (3)$$

where T_s is the torque generated by the shoulder and T_p is torque generated by the pin. Assuming that a uniform shear stress τ occurs during welding, we obtain

$$T_f = \int_{r_i}^{r_o} \tau(2\pi r) r dr + \int_0^{r_i} \tau(2\pi r) r dr + \tau(2\pi r_i h) r_i \qquad (4)$$

where r_o is the radius of the shoulder, r_i is the radius of the pin, and h is the height of the pin, as shown in Fig. 2. Equation 3 reduces to

$$T_f = 2\pi r_o^2 \tau\left(\frac{1}{3} r_o + \frac{r_i^2}{r_o^2} h\right) \qquad (5)$$

Assuming a coefficient of friction is μ, the total friction force F_f due to the compressive force F is given by

$$F_f = \mu F \qquad (6)$$

Noting that $\pi r_o^2 \tau$ is the total friction force, Eq. 3 yields

$$T_f = 2\mu F(\frac{1}{3}r_o + \frac{r_i^2}{r_o^2}h) \qquad (7)$$

Substituting Eq. 5 into Eqs. 1 and 2, we obtain

$$E_f = 2\mu F\left(\frac{1}{3}r_o + \frac{r_i^2}{r_o^2}h\right)\frac{\omega}{v_o} \qquad (8)$$

Equation 8 defines the energy per unit length of the weld due to friction between the tool and the workpiece. For a given tool geometry, tool speed, and workpiece material, this energy can be easily identified. As can be noted from Eq. (1), the power generated due to friction is given by

$$P_f = 2\mu F\left(\frac{1}{3}r_o + \frac{r_i^2}{r_o^2}h\right)\omega \qquad (9)$$

Frigaard [13] reported that the coefficient of friction between aluminum and mild steel should be set as the average value between 0.5 for sticky friction and 0.25 for dry sliding. Hamilton [12] used 0.5 as an initial value for the coefficient of friction, and then reduces it as the energy level increases. For instance, they reduced the coefficient of friction to 0.45 when the energy level exceeds 2000 J/mm and 0.4 for an energy level exceeding 3000 J/mm. In this study, a coefficient of friction of 0.5 is used.

The other source of heat is due to the plastic deformation within the workpiece. Provided that the plastic deformation within the workpiece is totally transformed into heat, the heat generated due to plastic deformation per unit weld length can be expressed as follows:

$$E_p = \sigma\, \varepsilon\, dV \qquad (10)$$

where σ and ε are the stress and strain, respectively, $dV = 2\,\mathrm{r_i} h$ is the volume per unit length of the material. The stress σ is given by

$$\sigma = K\varepsilon^n \exp\left(\frac{mQ}{R_G T}\right) \qquad (11)$$

where *K* is the strength coefficient, *n* is the strain hardening exponent, *m* is the strain rate sensitivity, *Q* is the apparent activation energy, R_G is a constant equals $8.32\,\mathrm{J\,mol^{-1}K^{-1}}$, and *T* is the absolute temperature. As a result, the energy generated due to plastic deformation per unit length of the weld is expressed as follows:

$$E_p = K\varepsilon^{n+1}\left(2\,\mathrm{r_i} h\right)\exp\left(\frac{mQ}{R_G T}\right) \qquad (12)$$

For Al 2024, the strength coefficient $K = 690$ and the strain hardening exponent is given by $n = 0.16$. The stress-strain relationship in the room temperature is shown in this figure.

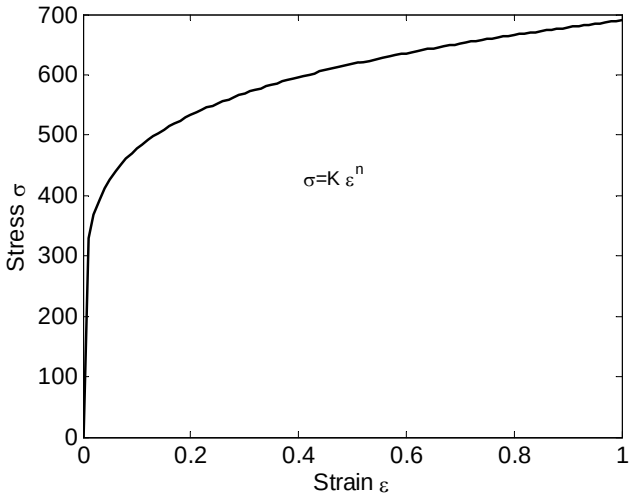

Fig. 3 True-stress true-strain curve for AA 2024.

Because the temperature is already unknown, the accurate calculation of the plastic strain energy needs an iterative process. Since the effect of the energy due to plastic deformation is much smaller than that due to friction, a simple model was proposed as follows:

$$E_p = \sigma_e \varepsilon_e \left(2\,\mathrm{r_i} h\right) \qquad (13)$$

where σ_e is the equivalent (effective) stress and ε_e is the effective strain. Using the finite element method, Heurtier et al. [3] found that the effective strain is around six. In this case, the effective stress is assumed to be constant, and hence the area under the curve becomes a rectangle. The power generated due to the plastic deformation is given by

$$P_p = \sigma_e \varepsilon_e \left(2\,\mathrm{r_i} h\right) v_o \qquad (13)$$

The total energy generated per unit length of the wild is the sum of the energy generated due to friction between the tool and the workpiece surface and the plastic deformation within the workpiece.

A scaling factor is introduced in order to control the effect of the energy due to plastic deformation. At low levels of heat generation, the plastic deformation plays a significant role. As the frictional heat becomes larger, the effect of the plastic deformation diminishes. Hamilton et al. [12] reported three regions based on the experimental results available in the literature. For energy levels below 800 J/mm, heat generation

due to plastic deformation dominates heat generation due to friction. For energy levels greater than 2000 J/mm, frictional slip occurs due to the material softening. In the region in between, both sources of heat are considerable. Based on that, the scale factor, as presented in Fig. 4, is proposed in this study.

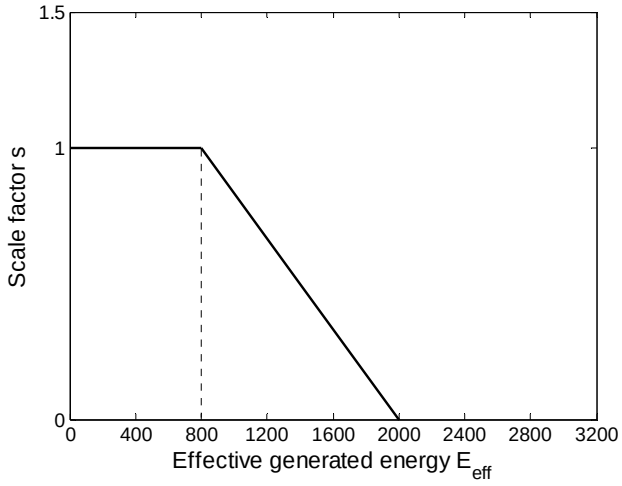

Fig. 4 The proposed scale factor to control the heat due to plastic deformation.

As a result, the total energy generated can be expressed as follows:

$$E = E_f + sE_p = 2\mu F\left(\frac{1}{3}r_o + \frac{r_i^2}{r_o^2}h\right)\frac{\omega}{v_o} + s\sigma_e\varepsilon_e\left(2r_i h\right) \tag{14}$$

where the scale factor *s* is shown in Fig. 4. The total power generated is given by

$$P = Ev_o = 2\mu F\left(\frac{1}{3}r_o + \frac{r_i^2}{r_o^2}h\right)\omega + s\sigma_e\varepsilon_e\left(2r_i h\right)v_o \tag{15}$$

The term effective energy is introduced to take into account the case where the height of the FSW tool pin *h* is different from the thickness of the workpiece *t*. The effective energy is defined as follows:

$$E_{\text{eff}} = \frac{h}{t}E = \beta E \tag{16}$$

where β is the coefficient of transfer efficiency.

III. Results and Discussion

The energy model proposed in the previous section accounts for both the frictional heating and the heating results from the plastic deformation. In order to validate the model, the total energy presented in our model is adopted into the empirical formula developed by Hamilton et al. They obtained this formula from the experimental results available in the literature. The empirical formula is given by

$$\frac{T_{\max}}{T_s} = 1.56\times10^{-4}E_{\text{eff}} + 0.54 \tag{15}$$

where $T_{\max}$ is the maximum temperature generated within the weld, T_s is the solidus temperature in Kelvin, E_{eff} is the effective energy generated per unit length of weld in J/mm as given in Eq. (15). They nondimensionlized the obtained maximum temperature so that the deduced formula can serve for the AA6000 and AA7000 series considered in their study. They obtained a good agreement except in the low-energy level region. The reason is that they neglected the energy generated by the plastic deformation, which is significant when the frictional heating is low. In our model, the heating due to plastic deformation has been taken into consideration through the scaling factor as given by Eq. (14). To validate our model, we find the total energy generated for given welding parameters and solve for the maximum temperature. The obtained maximum temperature is then compared to both the model given by Hamilton et al and the experimental results. It is found out that considering the heat due to plastic deformation enabled our model to better fits the experimental results at all energy levels. Next, we present our findings.

Four aluminum alloys are considered using different welding parameters such as tool geometry and welding speed. Table 1 presents the four alloys with the material characteristics and tool geometry used for each case.

TABLE I
MATERIAL CHARACTERISTICS AND TOOL GEOMETRY OF THE ALUMINUM ALLOYS USED.

Aluminum Alloy	6061-T6	6061-T651	6082-T6	7050-T7451	7050-T7451
Ref.	**14**	**15**	**13**	**16**	**10**
t(mm)	6.4	8.13	6.0	6.4	19.1
$\rho(\text{kg/m}^3)$	2700	2700	2700	2830	2830
c_p (J/kg K)	896	896	889	860	860
k(W/m K)	167	167	170	157	157
α $(\times10^{-5}\,\text{m}^2/\text{s})$	6.9	6.9	7.1	6.5	6.5
T_s (K)	855	855	879	761	761

Tool geometry	r_o mm	12.0	12.7	7.5	10.2	9.5
	r_i mm	9.5	5.0	2.5	3.6	3.2
	h mm	6.0	8.0	6.0	6.1	6.4

Welding parameters including the tool rotational speed, tool translational speed, and the acting normal force are given in Table 2.

TABLE II
WELDING ROTATIONAL AND TRANSLATIONAL SPEEDS AND THE APPLIED NORMAL FORCE.

Alloy	Welding parameters			
	Case #	rpm	v_o (mm/s)	F (kN)
AA6061-T6	1	344	2.2	13
AA6061-T651	2	390	2.4	22
AA6082-T6	3	1500	5	7
	4	1500	8	7
	5	1500	12	7
AA7050-T7451	6	180	0.85	20
	7	180	1.3	25
	8	180	1.7	28
	9	360	1.7	24
	10	540	2.5	34
	11	810	3.8	39
AA7050-T7451	12	520	1	18
	13	520	1.9	24
	14	700	1	13
	15	700	1.9	16
	16	700	2.6	18

TABLE III
ENERGY AND MAXIMUM TEMPERATURE OBTAINED USING OUR MODEL AND HAMILTON'S MODEL.

Case #	Welding properties				
	E(J/mm) Ref[12]	E(J/mm) Ours	T_{max} Exp.	T_{max} Ours	% Error
1	1639	1756	698	681	2.4
2	1896	2049	739	731	1.1
3	696	791	594	583	1.8
4	435	529	548	547	0.1
5	290	384	523	527	0.8
6	1845	1863	628	622	1.0
7	1513	1564	623	588	5.6
8	1273	1373	593	566	4.5
9	1978	1993	673	636	5.4
10	2464	2559	663	701	5.7
11	2868	2897	703	739	5.1
12	3053	3053	493	532	8.0
13	2410	2410	448	507	13.1
14	3710	2968	533	529	0.8
15	2403	2163	493	497	0.8
16	2229	1978	483	490	1.4

A comparison between the heat energy obtained by Hamilton et al. and the heat energy obtained using the proposed model in this study is given in Table 3. Investigating these results, one notes that at low-energy levels, for the first five cases for instance, the model of Hamilton et al. underestimates the generated energy. This is expected since the plastic deformation is significant in this region, which is ignored in their model. On the other hand, the energy predicted using our model seems much greater then theirs, which reflects the enhancement of the model by including the plastic deformation. Moreover, in the high energy level, up to 2000 J/mm, the results are very close. This yields the conclusion that the scale factor tunes the contribution of the plastic heat energy.

To validate these results, we determined the maximum temperature extracted from our model and compare it with the experimental results, which are given in Table 3. A good agreement is obtained at all energy levels. Moreover, the percentage error obtained in each case is presented. The error seems to be limited except for only one case, which reveals the possibility of inaccurate measurement. Variation of the maximum temperature normalized with the solidus temperature of the material with the effective energy using our model is shown in Fig. 5. The obtained results are compared with the experimental results. As shown in the figure, a good agreement was obtained at all energy levels. Figure 5 is the graphical representation of the data given in table 3.

Hamilton et al. [12] investigated the friction stir welding of AA6061-T6 having the tool parameters and welding conditions as given in Table 4. They used a simulation model that account for the heat transfer within and around the weld tool. They presented the calculated energy and the simulated maximum temperature. Comparing with the experimental results, their results fit well at high energy levels, while lack accuracy at low energy levels. As a revalidation of our model, we considered this case and obtained the generated energy and maximum temperature for each case. As can be noted from Table 4, the energy generated using our model is greater than that of Hamilton for energy levels up to 2000 J/mm. Figure 6 shows the variation of the normalized maximum temperature with the effective energy level. The results obtained using our model are in a good agreement with the empirical.

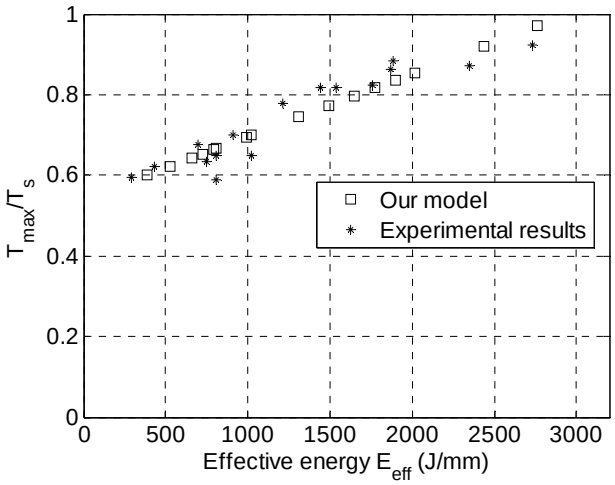

Fig. 5 Variation of the maximum normalized temperature with the effective energy.

TABLE IV
ENERGY AND MAXIMUM TEMPERATURE OF THE FSW OF AA6061-T6 AND A COMPARISON BETWEEN OUR MODEL AND HAMILTON'S MODEL.

rpm	Welding properties for AA6061-T6 $r_o = 12.7$ mm, $r_i = 5.0$ mm, $h = 8.0$ mm, $v_o = 2.4$ mm/s, $F = 22$ kN			
	E(J/mm) Ref[12]	E(J/mm) Ours	T_{max} Ref[12]	T_{max} Ours
50	333	643	398	547
100	664	971	479	591
175	1163	1432	570	653
200	1329	1562	594	670
225	1495	1692	615	687
250	1661	1822	635	705
300	1993	2081	667	739
350	2325	2341	691	774
450	2691	2660	758	816
550	3289	3251	776	895

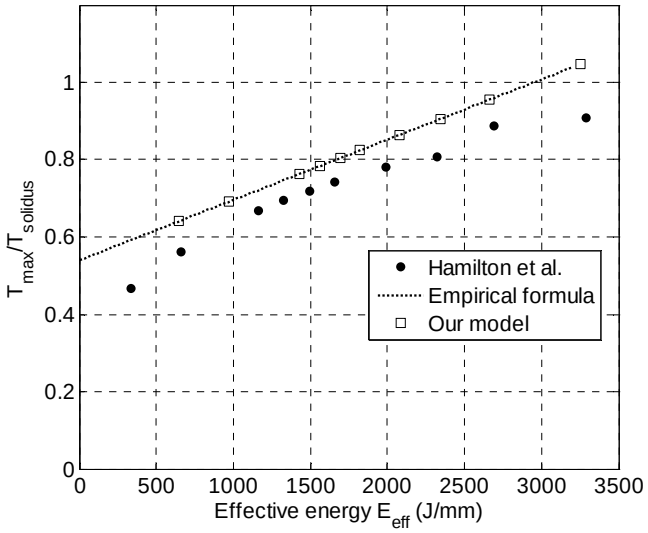

Fig. 6 Variation of the maximum temperature with the energy level for our model, Hamilton's model, and the experimental results.

IV. CONCLUSIONS

In this study, a simple model that estimates the energy generated in friction-stir welding is presented. The model accounts for the heat generated due to friction between the weld tool and the surface of the workpiece and heat generated due to plastic deformation. The later is scaled such that its effect becomes significant at low-energy levels. To account for the possible difference between the tool height and the thickness of the workpiece, a transfer efficiency coefficient is introduced in order to obtain an effective energy for the process. Based on an empirical formula that is based on experimental results, the maximum temperature in the weld is related to the effective energy. A comparison between the estimated heat energy and its corresponding maximum temperature obtained using the proposed model and the experimental results shows a good agreement. The heat due to plastic deformation is found to have a significant effect on the resulting temperature especially at low-energy levels. This model can be enhanced by considering an accurate model for the plastic deformation that will automatically predicts the heat generation due to plastic deformation at different energy levels. This will automatically eliminate the scale factor introduced in this study. Moreover, an accurate thermal model that simulates the heat transfer within and around the weld tool could be used.

REFERENCES

[1] W. M Thomas, "Friction Stir Butt Welding", International Patent Application PCT/GB92, Patent Application GB125978.8, 1991.

[2] The Welding Institute Website: www.twi.co.uk

[3] P. Heurtier, M. J. Jones, C. Desrayaud, J. H. Driver, F. Fontheillet, and D. Allehaux, "Mechanical and Thermal Modeling of Friction Stir Welding", Journal of Materials Processing Technology, Vol. 171, pp. 348-357, 2006.

[4] R. S. Mishra, and Z. Y. Ma, "Friction Stir Welding and Processing", Materials Sciences and Engineering, R 50, pp. 1-78, 2005.

[5] G. J. Bendzsak, T. H. North, and C. B. Smith, "An Experimentally 3D Model for Friction Stir Welding", 2nd International Symposium 'Friction Stir Welding', TWI Ltd., Gothenburg, Sweden, 2000.

[6] Askari, S. Silling, B. London, and M. Mahoney, "Modeling and Analysis of Friction Stir Welding Processing", K. V. Jata, et al. (Eds.), Friction Stir Welding and Processing, TMS, Warrendale, PA, pp. 43-54, 2001.

[7] P. Heurtier, C. Desrayaud, and F. Montheillet, "A Thermomechanical Analysis of the Friction Stir Welding Process", Materials Science Forum, Trans. Tech. Publications, Switzerland, pp. 1537-1542, 2002.

[8] S. Xu and X. Deng, "Two and Three Dimensional Finite Element Models for the Friction Stir Welding Process", 4th Int. Symp. On Friction Stir Welding, TWI Ltd., Park City, Utah, USA, 2003.

[9] P. Dong, F. Lu, J.K. Hong, and Z. Cao, "Coupled Thermomechanical Analysis of the Friction Stir welding Process using Simplified Models", Science Technology Welding and Joining, Vol. 6, pp. 281-287, 2001.

[10] P. Ulysse, "Three-Dimensional Modeling of Friction Stir Welding Process", International Journal of Machine Tools and Manufacture, Vol. 42, pp. 1549-1557, 2002.

[11] F. Palm, U. Hennebohle, V. Erofeev, E. Earpuchin, and O. Zaitzev, "Improved Verification of FSW-Process Modeling relating to the Origin of Material Plasticity", 4th Int. Symp. On Friction Stir Welding, TWI Ltd., Metz, France, 2004.

[12] Hamilton, S. Dymek, and A. Sommers, "A Thermal Model of Friction Stir Welding in Aluminum Alloys", International Journal of Machine Tools and Manufacture, Vol. 48, pp. 1120-1130, 2008.

[13] O. Frigaard, O. Grong, and O. T. Milding, "Modeling of Heat Flow Phenomena in Friction Stir Welding of Aluminum Alloys", Proceedings of the 7th International Conference in Joints in Aluminum, Vol. S16, 1998.

[14] P. A. Colgrove, and H. R. Shercliff, "Experimental and Numerical Analysis of Aluminum Alloy 7075-T7351 Friction Stir Welds", Science and Technology of Welding and Joining, Vol. 8, pp. 360-368, 2003.

[15] M. Z. Khandkar, J. A. Khan, and A. P. Reynolds, "Prediction to Temperature Distribution and thermal History during Friction Stir Welding: Input Torque based Model", Science and Technology of Welding and Joining, Vol. 8, pp. 165-174, 2003.

[16] P. A. Colgrove and H. R. Shercliff, "Three-Dimensional CFD Modeling of Flow around a Threaded Friction Stir Welding Tool Profile", Journal of Materials Processing Technology, Vol. 169, pp. 320-327, 2005
eted from the biography.